University of Groningen

Safety issues during surgical monitoring

Journée, H. Louis; Shils, Jay L.

Published in:
Intraoperative Neuromonitoring

DOI:

IMPORTANT NOTE: You are advised to consult the publisher's version (publisher's PDF) if you wish to cite from it. Please check the document version below.

Document Version
Publisher's PDF, also known as Version of record

Publication date:
2022

[Link to publication in University of Groningen/UMCG research database](#)

Chapter 5

Safety issues during surgical monitoring

H. LOUIS JOURNÉE[1*] AND JAY L. SHILS[2]

[1]Department of Neurosurgery, University Medical Center Groningen, University of Groningen, Groningen, The Netherlands

[2]Department of Anesthesiology, Rush University Medical Center, Chicago, IL, United States

Abstract

While intra-operative neuro-physiologic assessment and monitoring improve the safety of patients, its use may also introduce new risks of injuries. This chapter looks at the electric safety of equipment and the potential hazards during the set-up of the monitoring. The physical and functional physiologic effects of electric shocks and stimulation currents, standards for safety limits, and conditions for tissue damage are described from basic physical principles. Considered are the electrode-tissue interface in relation to electrode dimensions and stimulation parameters as applied in various modalities of evoked sensory and motor potentials as to-date used in intra-operative monitoring, mapping of neuro-physiologic functions. A background is given on circumstances for electric tissue heating and heat drainage, thermal toxicity, protection against thermal injuries and side effects of unintended activation of neural and cardiac tissues, adverse effects of physiologic amplifiers from transcranial stimulation (TES) and excitotoxicity of direct cortical stimulation. Addressed are safety issues of TES and measures for prevention. Safety issues include bite and movement-induced injuries, seizures, and after discharges, interaction with implanted devices as cardiac pacemaker and deep brain stimulators. Further discussed are safety issues of equipment leakage currents, protection against electric shocks, and maintenance.

INTRODUCTION

While intra-operative neuro-physiologic assessment and monitoring improve the safety of patients, its use may also introduce new risks of injuries. To appreciate these, it is important to be aware of the variety of safety aspects, understand their causes, and understand preventative measures. These subjects are described in this chapter by specifically looking at the electric safety of equipment, potential hazards during the set-up, and performance of monitoring.

ELECTRIC SAFETY

Neurophysiologic and other equipment in the operating room, as used by the surgeon and anesthesiologist, utilize "line" electricity to operate. All of this equipment is connected to the patient via various interfaces. Thus, there is the chance for dangerous electric currents to pass through the patient.

Electric connections with the patient

Electric connections consist of electrode connections, contact between patient and surrounding conducting parts of equipment, the operation table, and cables. The nature of the electric coupling is resistive, inductive, capacitive, or consists of radio-frequent transmission (RF) passage. 50 or 60 Hz AC currents may arise from leakage currents or faulty connections to the patient via supply lines. There are high current devices that are directly connected to the patients for therapy and include electro-cautery devices and electric stimulators.

---

*Correspondence to: Henricus Louis Journee, M.D., Ph.D., Neurosurgery, University Medical Center Groningen, University of Groningen, Groningen, The Netherlands. Tel: +31646574949, E-mail: hljournee@gmail.com

Effects of electric currents

There are two primary deleterious effects from electric currents passing through the patient: (1) physic effects from electric shocks and (2) functional physiologic reactions from electrically activated tissues.

ELECTRIC SHOCK

An electric shock consists of current passing through the body between two or more contacts. Electric currents may cause physic damage to tissues like burns and risk of cardiac failure. These depend on the current shape, strength, frequency, and location on the body where applied. Alternating currents between 10 and 200 Hz are most dangerous. This includes 50 or 60 Hz powerline frequencies.

FUNCTIONAL PHYSIOLOGIC ACTIVATION

Electric currents can also activate functional excitable tissues of the heart, muscles, and the central nervous system. This may interfere with existent physiologic functions. The effects range from perception to pain, muscle contractions, induced tissue damage, and convulsions.

Cardiac failure

Electric currents can also activate the heart muscle by eliciting triggering effects on heart rhythm, induction of brady- and tachycardia, atrial or ventricular fibrillation, and heart failure (Ponder et al., 2003; Morano and Tung, 2019). Fatal ventricular fibrillation with a probability of 100% will occur at a current from an intracardiac electrode of only 0.5 mA. The change drops to about 1% at 0.05 mA (NFPA 99, 2005; IEC 60601-1, 2012). The effects are negligible when alternative current intensities of 500 μA are applied at the surface of the patient. 50 or 60 Hz leakage current shocks could by accident be conducted via intravascular central lines to the intracardiac location and stimulate from there.

Cardiac arrhythmia when using pulse train transcranial electric stimulation (TES) occur rarely (MacDonald, 2002; MacDonald and Deletis, 2008) and could be caused by deep current penetration to autonomic centers and by a "parasitic" current pathway through scalp somatosensory potentials (SEP) electrodes to leg electrodes through the heart and back to the head as described in Section "TES-induced parasitic current conduction along with physiologic amplifiers."

Conditions for electric activation of the heart muscle and nerve tissues

Electrically excitable tissues like heart muscle fibers and axons can be activated by external currents. These originate at the electrode contact surface starting with high current densities penetrating the volume conductor and then spatially decreasing rapidly. This is illustrated in Fig. 5.1A and B. The electric field $\vec{E}$ is maximal in the current direction, which is horizontal in this model. $\vec{E}$[V/cm] (the electric field) is, according to $\rho \cdot j$, linearly related to the current density j [A/cm^2] where ρ is the specific resistance [Ω cm]. Electric elicitable tissue fibers are maximally activated when oriented in the direction of the field. *Activation of electric elicitable tissue fibers is only possible when the projection of the electric field $\vec{E}_a$, varies along the fibers* (Rattay, 1986). The variation of the electric field, $\Delta\vec{E}_a$, over a distance Δa between neighboring points on the fiber is the field gradient $G_a = \Delta\vec{E}_a / \Delta a$ [V/cm^2]. The set of G_a values along axon or heart muscle fibers defines an activation function (Rattay, 1986). Positive values are regions of fiber depolarization while negative values are regions of fiber hyperpolarization. *When $G_a = 0$, no activation will occur, even when electric fields are high*. The activation functions along the fiber are depicted in graphs C and D of Fig. 5.1.

Normally excitable tissue fibers that are insensitive to stimulation are at the midpoint between the stimulation electrodes due to (1) current densities and $\vec{E}$ values are minimal—not necessarily zero—and (2) activation is zero at the transition from depolarization into hyperpolarization. This is at the intracardial location in Fig. 5.1A. The high activation thresholds of transthoracic AC currents of 500–1000 μA make the heart function robust against relative high currents that enter at the skin surface and are considered safe according to the International Electrotechnic Commission (IEC) safety standards.

In contrast, the activation function and $\vec{E}$ are maximal and the yield lowest stimulation thresholds at the location of the electrodes. This occurs also at intracardial current stimulation location (Fig. 5.1B) where intracardiac stimulation current thresholds are as low as 50 μA.

However, one has to be aware that in practice, the volume conductors in Fig. 5.1 consist of many tissue compartments, like lungs, mediastinum, skin, fat, and different muscles, each having their own specific conductivities and geometry. The transitions from relatively high to low conductivities such as from blood to the heart muscle introduces local variations of the electric field which implies there are non-zero activation functions even at the geometric midpoint between the electrodes. Thus, intracardiac stimulation may be effective at cross-thoracic currents in the magnitude often of milliamperes. This may disturb the heart rhythm in SEP recordings and even may cause cardiac arrest (Morano and Tung, 2019). Although very rare, transcranial stimulation is reported to cause bradycardia (Ponder et al., 2003) or affect the heart rhythm as shown in Fig. 5.2 in our own experience.
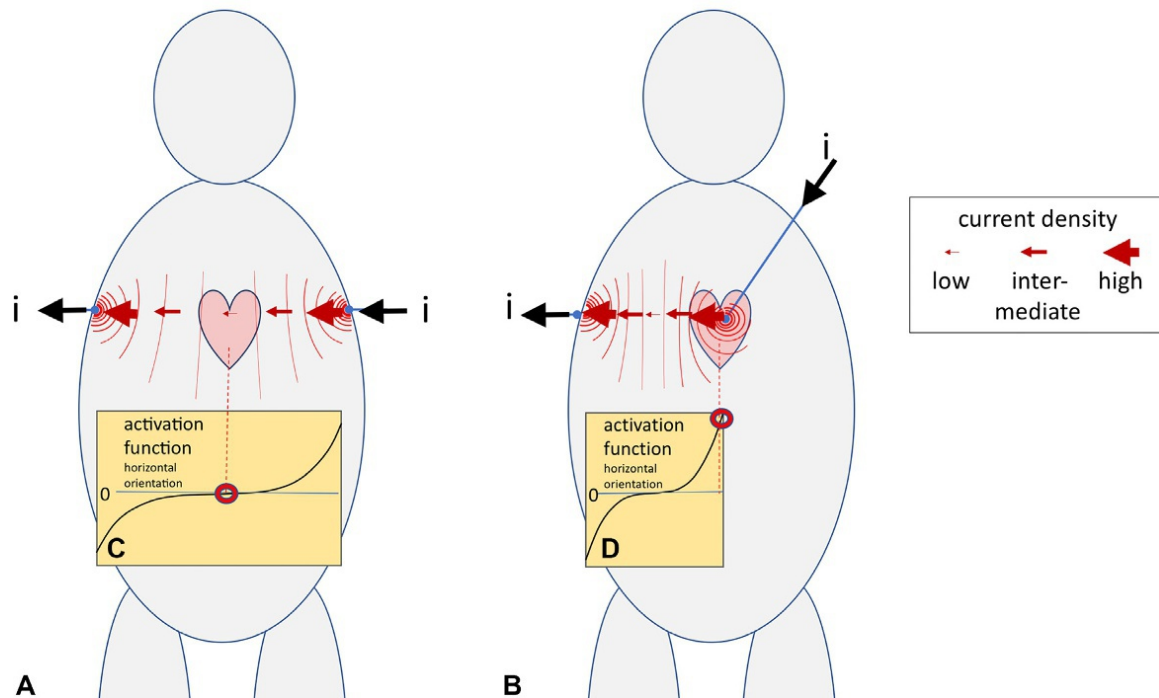
Fig. 5.1. Graphical representation of a volume conductor model, the human body when external currents are applied between: (A) two electrodes at the surface bilateral from the heart and (B) a combination of surface and intra-cardial electrodes. The curved lines show the distribution of isopotential planes at fixed potential steps. Densely distributed lines represent high electric fields $\vec{E}$ being maximal in the current direction. The width and direction of the arrows indicate current density and direction. Graphs (C) and (D) are the activation functions for horizontal oriented electric elicitable tissue fibers for models (A) and (B). The *red circles* show at intra-cardial location zero activation for externally applied currents and high activation at intra-cardial stimulation.
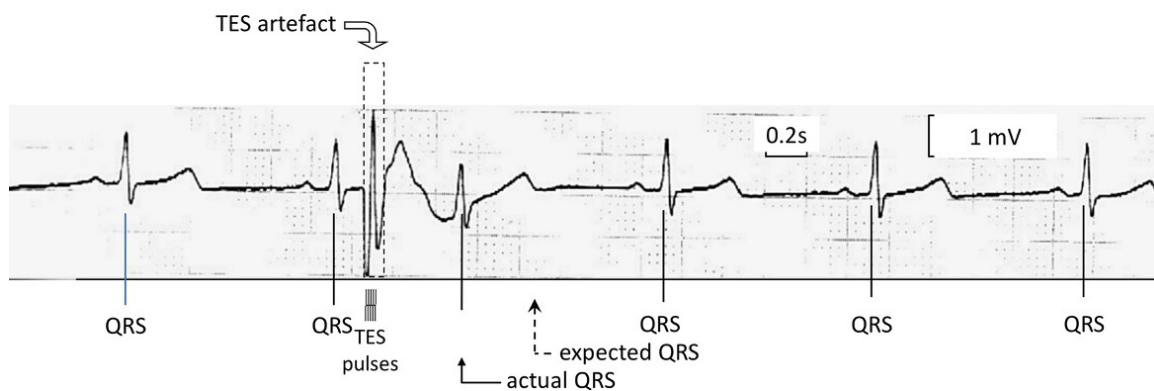

Fig. 5.2. Example of a negative influence of multi-pulse trans-cranial electric stimulation (TES) on a regular pacing heart, with a preset of a QRS wave followed by a regular R-R rhythm. The artifact from a high-frequency TES train is depicted in the ECG. Voltage TES: mono-phasic; anode: Cz anode; cathode: conductive strip on the forehead; pulse width 0.1 ms; inter-pulse interval 2 ms.

Physic effects of electric currents in general

Physic effects from electric currents may also cause reversible and irreversible tissue damage.

ELECTRIC HEATING

Most electric-induced tissue damages like burns are from electric heating. All electric currents in tissues with specific resistances of ρ, such as from stimulation pulses or cautery, dissipate energy. The highest energy dissipation occurs at locations with the highest current densities j [A/cm^2]. As depicted in Fig. 5.3A, the dissipated energy ΔW in a volume element $\Delta G = a\Delta \times S$, where S [cm^2] is the cross-section in an equipotential plane and Δa [m] a narrow distance between two enclosing equipotential planes, is:
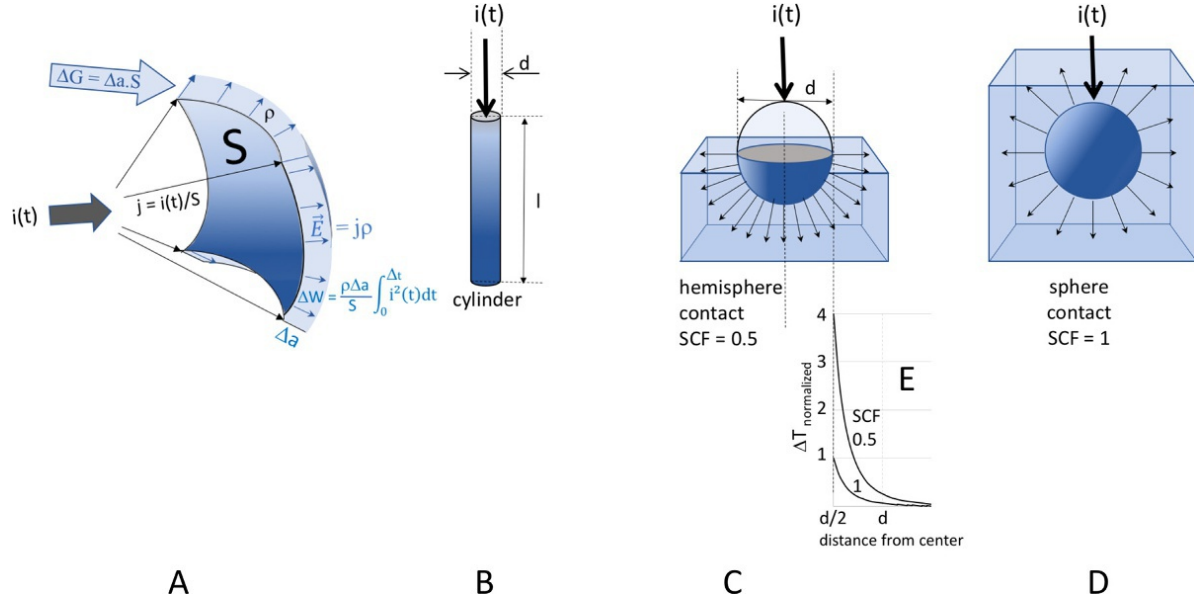
Fig. 5.3. Geometric models for computations of the dissipated electric energy in a volume conductor near the conductor surface. (A) Arbitrary equipotential plane with surface S adjacent to a thin shell with thickness Δa and volume ΔG in a volume conductor. (B–D): specific surface geometries of (B) a cylindric needle electrode, diameter d; length l, (C): hemispheric and (D): full sphere contacts of ball-tip electrodes with diameters d. i(t): current supplied to the contact surface, j: current density, SCF: surface coverage factor. The current density of a hemispheric contact surface is twice of a sphere, while the ΔT of the dissipated power ΔW at the surface is four times higher. This is depicted in graphs (E) where ΔT at SCF $= 1$ and 0.5 declines rapidly from the sphere surfaces.

$$\Delta W = \int_0^{\Delta t} i2(t).dt.\,\rho\,.\Delta a/S\,[J] \qquad (5.1)$$

where i(t) is the time function of the current and Δt is the exposure time of the current.

The highest current densities are found in the direct vicinity of the electrode contacts. These attenuate and spread out in the tissues according to spherical equipotential planes around a spherical electrode (Fig. 5.3C and D) and cylindric around a needle electrode.

The time function of the temperature increase ΔT (t) [°C] of the tissue adjacent to a *spherical electrode* surface with diameter d is:

$$\Delta T(t) = \int_0^t i2(t).dt.\,\rho/\left(SCF^2.C.\pi^2.d^4\right) \qquad (5.2)$$

where C is the heat capacity of the tissue [J.cm³/°C] and SCF is the tissue surface coverage factor being the tissue-covered part of the whole electrode surface. An SCF $= 0.5$ for a hemispheric coverage causes four times higher temperature increase than a full sphere as shown in Fig. 5.3E.

The temperature increase time function for a *cylindrical electrode* with subcutaneous length l and diameter d is:

$$\Delta T(t) = \int_0^t i2(t).dt.\,\rho/\left(C.\pi^2.d^2.l^2\right) \qquad (5.3)$$

This applies to needle and corkscrew electrodes.

These equations pertain to all kinds of electric currents like AC leakage currents, high-frequency cautery, and electric stimulation.

When currents are a series of undistorted rectangular waves where i(t) = i = is constant within the pulse width of each phase, then $\int_0^t$ i2(t). dt in Eqs. (5.1)–(5.3) can be replaced by:

$$m.i^2.n_m.np.pw$$

where, m is the number of trains (1 single train; 2 double train; >2 multitrain), i is current, n_m is the number of pulses in a train indexed by m, np is the number of phases (1: monophasic; 2: biphasic), and pw the pulse width.

Influence of electrode insertion

After subcutaneous insertion of the needle electrode, a thin fluid film may develop around the needle from a mechanically induced inflammatory response. The resistivity of the fluid is similar to interstitial fluid and is lower than the resistivity of surrounding tissue. In our experience, this fluid layer can cause up a maximum 20% decrease in electrode impedance. This high conductive fluid layer causes a virtual increase of the contact surface. The effective electrode diameter becomes $d + d\Delta$

where Δd is the enlargement of d. Then ΔT becomes smaller by a factor $[d/(d+d\Delta)]^2$. When Δd of a liquid film is 0.2 mm around a 0.4 mm diameter needle electrode, ΔT is reduced by 75%.

Heat drainage

The temperature increase is also reduced by heat drainage. One can distinguish three drainage principles:

(1) The fastest acting mechanism is heat conduction where the generated heat in the tissue near the electrode surface is conducted into the metal and also into the tissue. As deduced from Carslaw and Jaeger (1959) the heat transfer can be described by the heat conduction equation:

$$C\,\partial T/\partial t = \nabla\,(k.\nabla\,T) + PD \qquad (5.4)$$

where T is the tissue temperature (°C), t the time (s) and PD is the administered power density. Since the thermal conductivity k of stainless steel is around $\sim$ 15 W/(m.°C) is considerably higher than tissues such as gray, white matter and skin are 0.55, 0.48, and 0.37 W/(m.°C), respectively. The time function of the temperature course is the impulse response function h(t) and characterizes the heat draining effect. The bi-exponential temperature curve is characterized by an initial steep decrease from the electrode metal and transits into a moderate decrease from a compartment of a tissue compound. The onset of h(t) is defined at the onset of a very short pulse (δ-function) at t =0. The temperature course of the tissue including heat drainage ΔTH(t) can be computed as the convolution of any time function of the temperature course without heat drainage ΔT(t) and h(t):

$$\Delta TH(t) = \int_0^t \Delta T(u).h(t-u)\,du \qquad (5.5)$$

The applied electric power that is administered to the electrode applies to RF and stimulation sources. A δ-function can be approached by flash RF pulses of short duration. Fig. 5.4 is deduced from graphic data of Cosman and Cosman (2005) and shows three temperature clearance curves obtained from temperature measurements at a cylindric electrode tip after administration of RF flash pulses of 10 ms duration at three intensities. Deduced time constants were estimated at $\tau = 7$–9 ms and $\tau = 40$–60 ms for the fast and slower components of the temperature clearance curve. The respective heat clearance rates are 11%–14%/ms and 1.5%–2.5%/ms for the tissue compound. Estimated exponential courses of the fast (1)

and slow (2) components are drawn in the three clearance curves. Deviations are possible when tissues are composed of different compartments introducing a modest multi-exponential distortion. Thus one can see how heat dissipation varies between different tissues.

(2) A significantly slower heat draining mechanism is clearance by blood perfusion. The cooling is proportional to the tissue perfusion rate and ΔT. The heat transfer rate (perfusion) are for brain, gray and white matter, and skin, respectively, 0.56, 0.74, 21.2.and 0.11 mL/min.g (deducted from ITIS database, 2019a). This means a heat clearance from blood perfusion of, respectively, -0.93% and -0.18%/s for brain and skin.

(3) A third heat drainage mechanism is radiation to the environment. The heat radiation is proportional with the surface of uncovered parts of the skin or brain and the temperature difference between the tissue surface and air.

THERMAL TOXICITY

An understanding of heat-induced tissue damage, specifically related to the brain and nervous tissue has been gained since the introduction of thermally induced lesions in the brain for the treatment of movement disorders and pain-related syndromes in the 1950s. Conditions for reversible and irreversible tissue damage are well-reported and based on temperature-controlled heating. The goal is to apply RF heating power into the tissue to bring the temperature of the targeted tissue above 45–50°C for a time duration of over 20 s by which cells will be destroyed. This is referred to as the "lethal temperature range" (Cosman and Cosman, 2005). Below this temperature range, permanent tissue damage is unlikely. A temperature setting of 45°C at duration times of larger than 30 s is often used as a test "lesions" since neural functions are temporarily ceased and predict effects of subsequent permanent lesions at higher temperatures. These disturbances are followed by a complete recovery.

Lesioning through deep brain stimulation (DBS) leads has also been investigated. When currents are administered through the Medtronic 3387 DBS electrodes of 1.5 mm length and 1.27 mm diameter over 60–120 s, no visible lesions are produced below 25 mA with a power of 0.5 J/s (Strickland et al., 2013). Oh et al. (2001) could not produce lesions with currents below 25–45 mA. Bourdillon et al. (2016) could not produce lesions below 0.5 J/s or 25 mA during 30 and 120 s continuous stimulation. Lesions were found when stimulating with RF power above 0.94 J/s for 30 s in a current range of 32–58 mA. Permanent lesions become evident
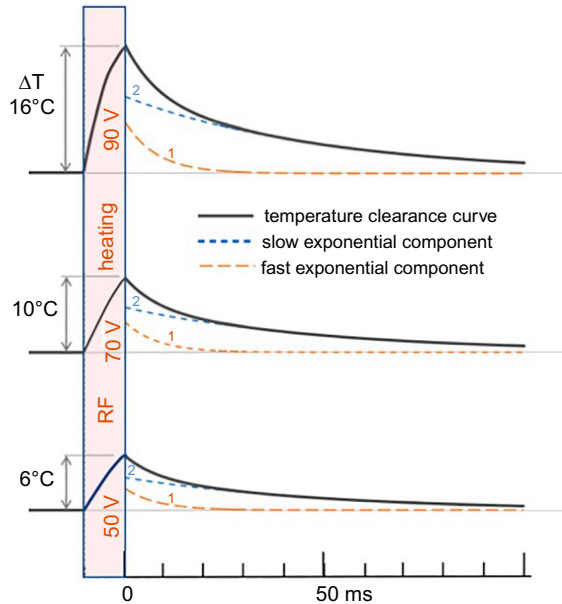
Fig. 5.4. Temperature clearance curves measurements from a cylindric electrode tip, 5 mm × 0.7 mm diameter during and after a 10 ms short RF power flash at three different voltages. For a 300 Ω impedance, the administered power at 90, 70, and 50 V is, respectively, 29, 16, and 8 W. The curves are deduced from the data of Cosman and Cosman (2005) and approximated by a bi-exponential curve being composed of fast (1) and slow (2) decreasing exponential time functions. The mismatch at the tails of the original graphs (not shown) is likely from a deviation from a mono-exponential course of time function 2 by rather a multi-exponential course due to a composition of the tissue by more than a single compartment with a fixed time constant.

at >45 mA while 75 mA continuous RF was applied to secure permanent lesions (Oh et al., 2001; Strickland et al., 2013).

From the literature discussed, a continuous RF current of 25 mA at a maximal exposure time of 15 s seems to be the safety limit below which no neural tissue damage can be expected.

PROTECTION AGAINST THERMAL INJURY

The most likely location of thermal tissue damage from burns is at areas near the stimulation electrodes where current densities and local electrode impedances are high. The current densities rapidly disperse in the surrounding tissues as depicted in Fig. 5.3. An empirically determined safety limit, that has taken hold in the literature, is 50 mJ (IEC60601-2-40, 2016). This number is somewhat nebulous since it has no relation to safety if not associated with a time of application to generate the thermal effects.

Specific effects from stimulation

Stimulation is intended to activate neural or muscle tissues in order to perform specific measurements. Various energy modalities have "safe dosage" windows a minimal chance for tissue damage. This damage can be due to: (1) a direct physical impact of the stimulus energy causing local thermal effects, (2) adverse physiologic effects like epileptic seizures and modulation of blood pressure and (3) other side effects from related actions such as bite injuries from masseter muscle contraction. The most important stimulation modalities are discussed in this section.

TEMPERATURE EFFECTS

As mentioned above one safety concern of TES is induced temperature increase related damage, which is related to the intensity of the stimulus and the duration of application. According to Eq. (5.3), ΔT depends on the combination of stimulation parameters and electrode dimensions. Using common TES voltage stimulator outputs of pulse trains of 8 biphasic pulses per train (ppt), pulse width 75 μs/ phase, and a 1000 mA current. The temperature at the surface of the smallest used subdermal electrodes of 1.3 cm long, 0.45 mm diameter will then increase by 1.45°C, 1.78°C, 1.79°C, and 1.68°C for environments of water, muscle, skin, and nerve when using tissue conductivity values between 0.1 and 10 kHz (Faes et al., 1999) and heat capacity values (ITIS database, 2019b). $\Delta T = 1.8$°C is an upper limit of these values and can be considered as worst case and is depicted in the isotherms as a function of the electrode dimension parameters as shown in Fig. 5.5.

The temperature effects from a single train are well below 40°C.

Therefore, all subdermal electrodes that currently are applied for single train TES can be considered safe. For double trains with two times 8 pulses/train, ΔT will be doubled 3.6°C which still keeps the tissue temperature below 45°C. This temperature may be approached in multitrain TES, which recently is used for monitoring (Tsutsui et al., 2015; Tsutsui and Yamada, 2016). The stimulation timespan Δt of multitrains may extend to over several seconds. The temperature increase will be n-fold of ΔT of a single train. Corkscrew and small needle electrodes could become critical for excitotoxic effects under the worst-case conditions in Fig. 5.5.

One potential risk of burns from TES pulse trains may be the reduction of electrode contact surface when electrodes dislodge. According to Eq. (5.3), the temperature rise increases by the square of the sub-dermal fraction of the electrode length. According to Fig. 5.5A, for small needle electrodes of 13 mm length, ΔT inclines

instantaneous temperature rise of tissue at contact surface of different needle electrode dimensions

absent heat drainage
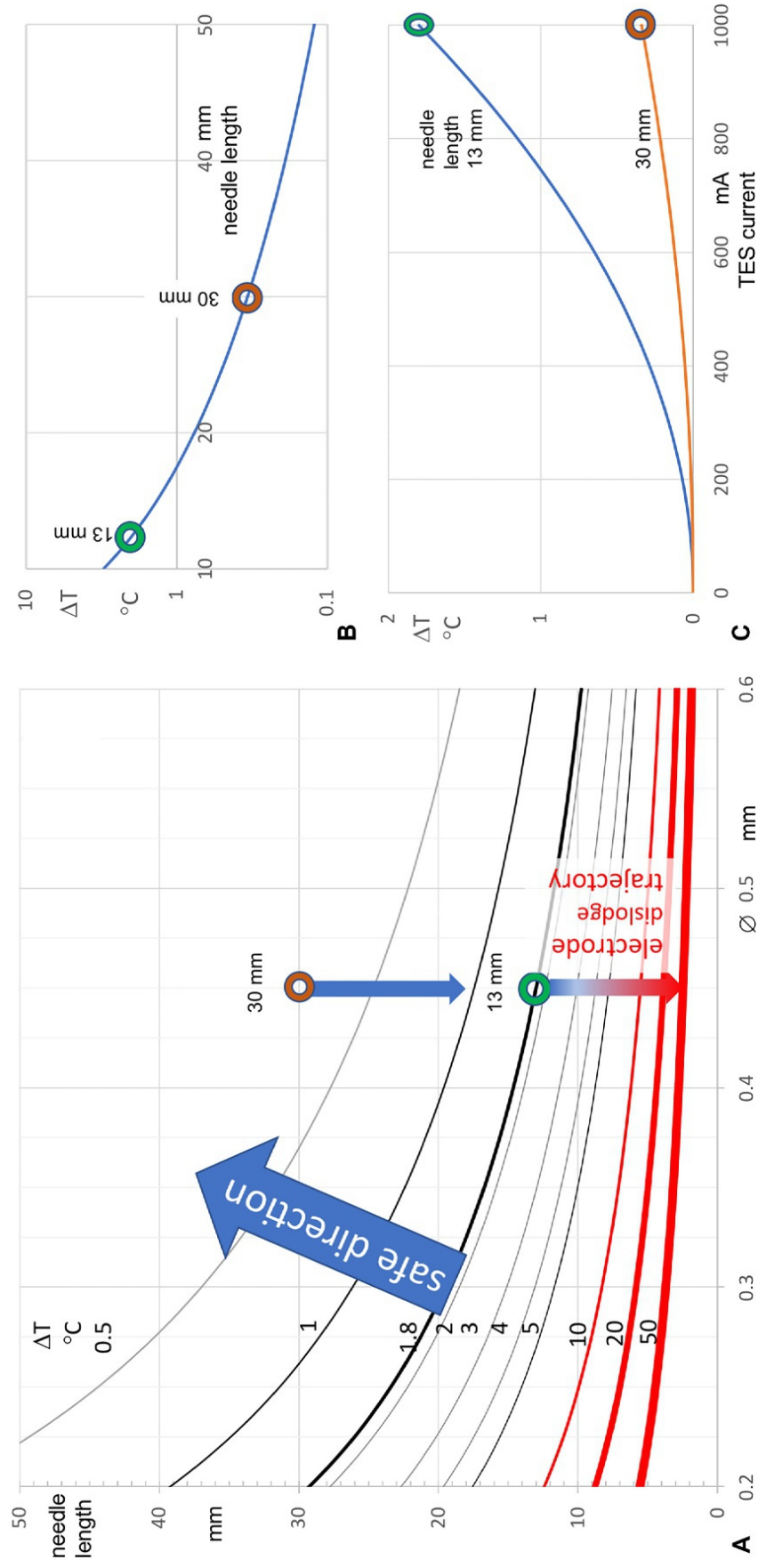
Fig. 5.5. (A) instantaneous temperature rise of tissue against contact surface sc needle electrodes at different dimensions of needle lengths and diameters. The thick black isotherm $\Delta T = 1.8°C$ refers to a worst-case TES condition: 8 biphasic TES pulse train, 75 μs/ phase, 1000 mA. The circles apply to a large contact surface electrode of 30 and a 13 mm electrode (approaches length corkscrew electrodes). The *vertical arrows* depict the increase of ΔT due to a gradual decrease of the inserted length. (B): ΔT as a function of diameter diameters, (C): ΔT as a function of the TES current.

rapidly up to over 50°C. This is less likely for 30 mm large contact surface electrodes. The temperature rise applies to a 0.2 mm thin tissue film around the inserted part of the electrode. If this needle is not all the way in the skin this reduction is less and the chance of a burn developing increases. At the same time, the electrode impedance may increase to over 1 kΩ (Journée et al., 2004; Berends and Journée, 2018). This is a self-limiting mechanism where the high electrode impedance limits the current and counteracts the high-temperature rise by the surface reduction. It is advised to secure the position of subcutaneous needle electrodes and to regularly check impedances or warnings of voltage or current limits. One should consider the dimensions of subcutaneous needle electrodes of 1.3 mm length and 0.4–0.45 mm diameter as minimum choices.

EFFECTS OF HEAT DRAINAGE

The temperature rise near the electrode will dissipate very quickly by conductive heat transfer as shown in Fig. 5.4. A heat drainage of −5%/ms becomes already evident within the short "flash" lengths where ΔT is for 20 ms 1.6 times larger than for 10 ms instead of the expected two times when heat conduction transfer is absent. The study of Cosman and Cosman (2005) showed that the heat conduction spread out to over 1 mm from the electrode.

According to Eq. (5.5), the temperature rise, ΔT, at the end of a pulse train will be reduced by more than 99% after 0.5 s instead of 0% without heat drainage. The effective exposure times to elevated temperature remain well below 0.1 s, which is more than two magnitudes lower than the times over tens of seconds that are necessary to develop any tissue lesions.

ACCURACY OF STIMULATORS

Specified stimulation parameters may be quite different in practice and depend on the type and brand of stimulators and may be important for reliable determination of stimulation thresholds. This may complicate comparisons between different brands of equipment. The current and voltage outputs of these stimulators are not necessarily constant. Initial currents may show peaks, reveal rebound effects after cessation of pulses or show compensating exponential effects from a charge balancing capacitor. Distortions of voltage pulses may depend on the load impedance. For example, the Digitimer™ D185 constant-voltage pulses show negative exponential rising currents followed by a post pulse exponential decay (Fig. 5.6G and H) (Journée et al., 2003).
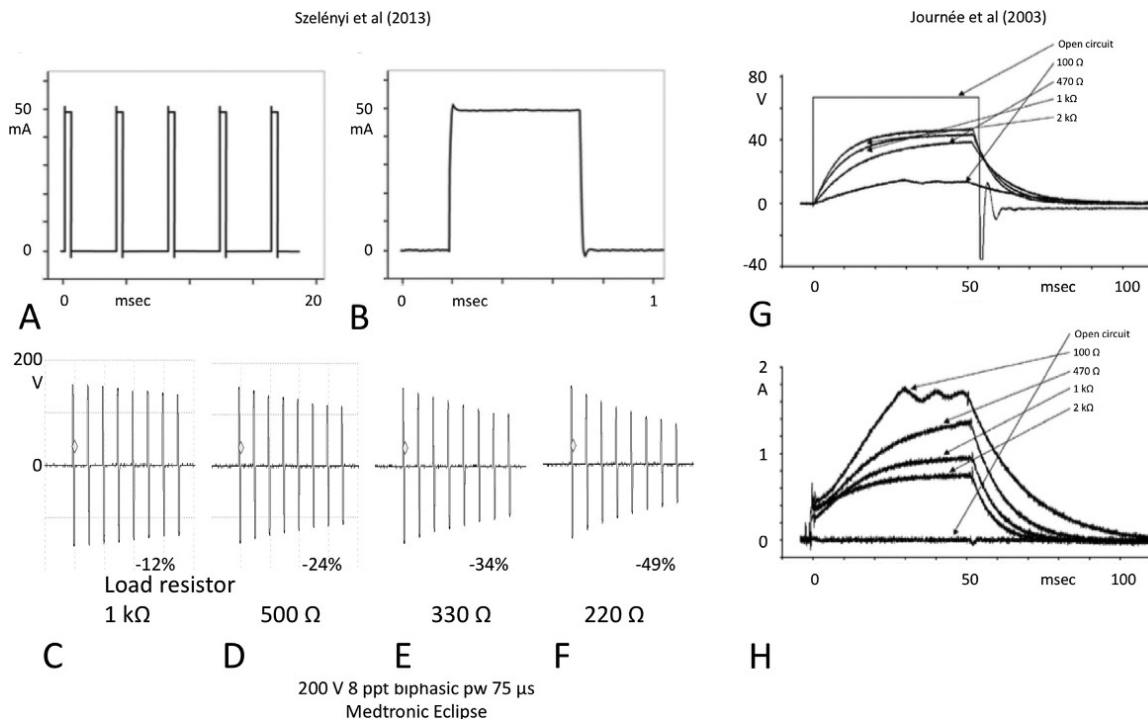
Fig. 5.6. Waveforms of current and voltage pulse trains of common brands of TES stimulators: (A) and (B) are current trains of a current stimulator of Inomed at a setting of 50 mA (Szelényi et al., 2013), (C–F): current waves of the Eclipse voltage stimulator of Medtronic with a voltage setting at 200 V showing the decay over pulse trains at increasing load impedances (unpublished data), (G) and (H) are simultaneously measured voltage and current shapes of the Digitimer D185 stimulator at different load impedances, showing strongly distorted monophasic square waves (Journée et al., 2003).

The Medtronic Eclipse™ transcranial voltage stimulator shows reasonable square wave pulses but reveals in trains of 8 pulses load dependent decays of -12% to -49% when load impedances decrease from $1\,k\Omega$ to $220\,\Omega$ (Fig. 5.6C–F). The lower impedances between 220 and $500\,\Omega$ apply to the low impedances of large contact surface electrodes. Their stimulation thresholds are less dependent on local electrode impedances when compared to small contact surface electrodes such as corkscrew and small needle electrodes (Journée et al., 2004; Berends and Journée, 2018). When no isolation transformers are used in the output circuit, current stimulators usually deliver reasonable undistorted square waves and the delivered currents agree with the current settings (Fig. 5.6A and B), except when voltage limits are reached.

At low load impedances and high intensities, the delivered voltages from transcranial voltage may be significantly lower than the settings. Estimated temperature effects will then be marked lower as expected, which is in favor of better safety. Measured TES thresholds depend on the brand of the voltage stimulator and can only be used for relative comparisons. Absolute thresholds can be obtained after calibration by actual measurements of delivered stimulation voltages and currents.

OPTIMIZATION OF THE PULSE WIDTH

Lower stimulation intensities are possible at an optimized pulse. At a rheobase of $200\,\mu s$ stimulation thresholds are about 30%–35% lower when compared to the 50–$75\,\mu s$ of voltage stimulators and often used $500\,\mu s$ of current stimulators (MacDonald et al., 2013). This may be helpful when stimulation intensity becomes a critical safety factor.

TES-induced parasitic current conduction along with physiologic amplifiers

A common issue when performing MEP and SEP monitoring is that the stimulus artifact can be greater than when not performing both modalities in the same patient. This occurs even when modalities are run independently of each other. This happens when SEP and EEG electrodes are placed close to TES electrodes. The scalp then may transduct voltages of over $100\,V$ from the stimulation electrodes via the SEP and EEG electrodes to the inputs of the physiologic amplifiers. Physiologic amplifiers are protected against electrostatic discharges (ESD) by current sinking circuits at their inputs. These become active above a given voltage level. When these circuits are activated, the normally high input impedance as seen by the electrodes becomes low impedance. This creates a connection to the isolated ground as shown in Fig. 5.7A and B for anodic and cathodic TES. Without an isolated ground connection, the currents are drained

by the inputs of several other amplifiers to the patient (Fig. 5.7C). Voltage levels at the high to low impedance transitions in various tested brands and types of equipment and instrumentation amplifiers vary between ±3 and $\pm20\,V$ Unpublished bench testing results by HLJ at $100\,V$ (direct or extrapolated) demonstrated leak currents of 10–$100\,mA$.

A parasitic current is caused by the fact that when two conductors at different potentials are close to one another, they are affected by each other's electric field. Current flows through the path of least resistance and thus when the input impedance of the amplifier drops this then becomes the most likely path. The low impedance state creates a gateway for the parasitic TES leakage currents from the head via the amplifier circuits in the patient box and isolated ground (Fig. 5.7A and B) or to the EMG electrodes when a ground connection is absent (Fig. 5.7C). The backflow of the TES-induced current via the legs can be as high as several tens of milliamperes and may re-trigger ECG pacing as shown in Fig. 5.2. However, this effect is expected to occur rarely for a similar reason as depicted in Fig. 5.1A.

Similarly, parasitic circuit gateways are possible *during monopolar cautery*. Since parasitic currents over $45\,mA$ are possible, this may create conditions for continuous cautery currents over 30–$60\,min$ to cause skin burns at the electrodes. As discussed, skin burns in EMG and stimulation electrodes are unlikely in TES. During periods of excessive cautery is it recommended to shut the amplifiers off to minimize the chances of this effect.

PREVENTION OF PARASITIC CONDUCTION

When combined SEP-MEP monitoring has to be performed with one machine, a switch box can temporarily disconnect the EEG SEP electrodes from the input amplifiers during TES to block parasitic TES currents as shown in Fig. 5.7D. It is advised to place the isolation ground of the EEG amplifier box away from the heart region, preferably near the head, like in the neck. Using this switch during monopolar cautery is recommended as well.

Some machines have isolated preamplifier boxes of which one can be used for EEG recordings and the other for electrodes elsewhere on the body. The boxes should be kept electrically isolated from each other. It is advisable to be alert for arrhythmia (MacDonald and Deletis, 2008). It is advised not to use monopolar cautery in the neighborhood of measurement or ground electrodes and to use bipolar cautery instead.

TES in skull defects and neonate anatomy

The brain is surrounded by three layers along which the currents from TES are distributed. These are a relatively well-conducting scalp, a relatively poor conducting
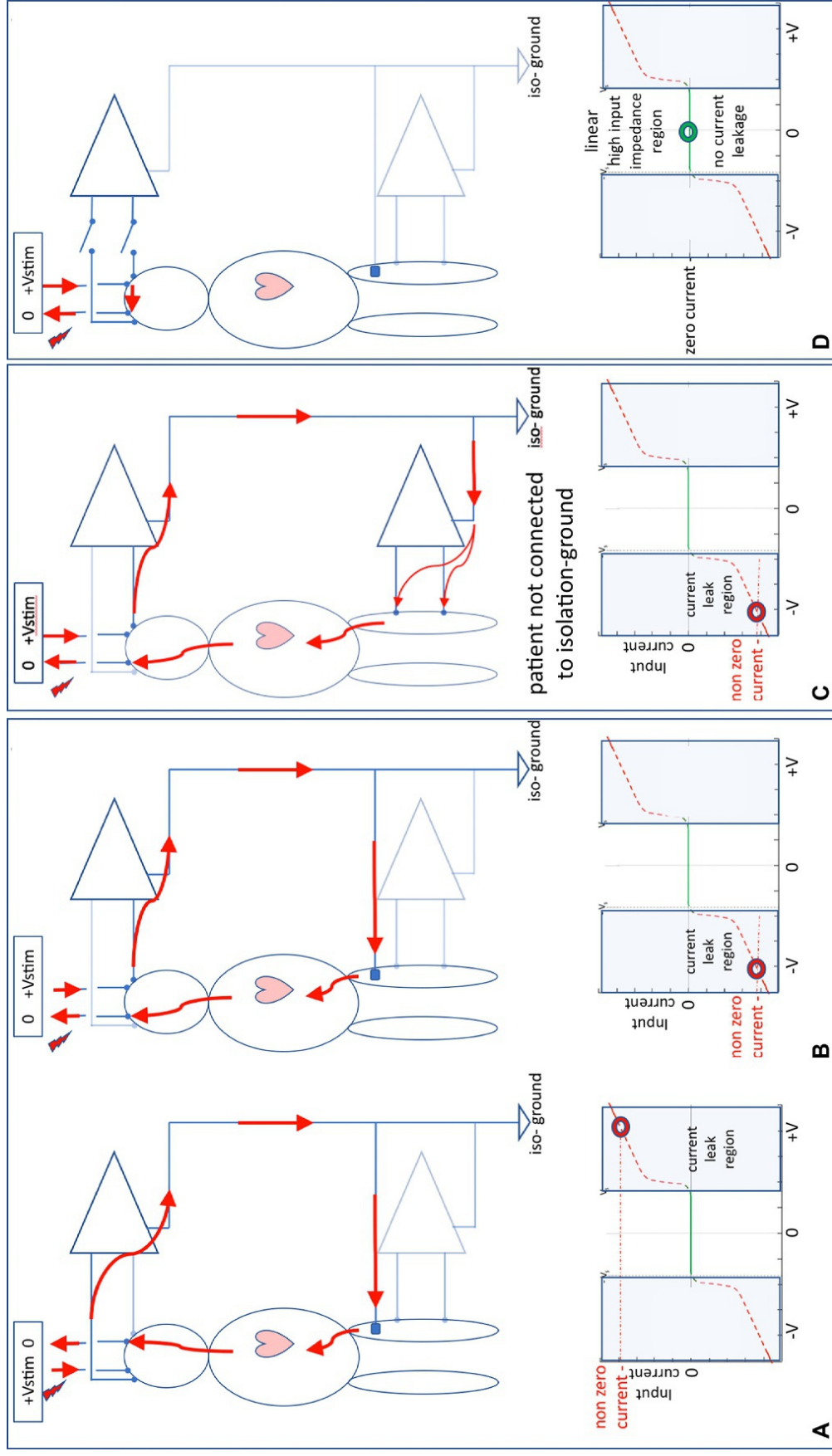
Fig. 5.7. TES current leak pathways via an EEG electrode to the input of an amplifier to the isolation ground and via the body back to the stimulator. (A) monophasic; C4 anode, (B) C3 anode. (C) C3 anode no isolation ground connection with the backflow of the current conducted along with the amplifier inputs and (D) prevention of TES current leak by disconnection of the SEP amplifier. The plots below are I–V graphs of one input of the SEP amplifier to the isolation ground. The *circles* mark the given situation.

skull, and well conducting cerebrospinal fluid (CSF). The third is natural protection against mechanical impact from outside. Much of the administered current from TES will be shunted by the first and third layer leaving a fraction to stimulate axons in the brain. Although activation functions, which express the excitability of axons, are not 1-to-1 related to $\vec{E}$ fields, but instead are first-order spatial $\vec{E}$ derivatives vector projections on axon courses, one should assume a very rough inverse relationship between current densities and motor thresholds. Under this assumption, the fractions of current densities are also reflected in the TES currents thresholds as opposed to direct cortical stimulation (DCS). The current density drops due to shunting in interposed layers and distance to the brain. Transcranial motor thresholds are therefore higher than at DCS. The TES thresholds of closer placed electrodes are higher, for example, C1–C2 vs C3–C4 (58 vs 40 mA, Szelenyi et al., 2007). Szelenyi (2013) showed current thresholds of 54.2 ± 22.8 and 13.5 ± 5.9 mA for TES and DCS. This would imply ratios of 1/4th to 1/5th. In our experience with deep brain stimulator leads, motor current stimulation thresholds near the corticospinal tract are on the order of 1–3 mA. This denotes ratios around 1/25th.

The skull has conductivities of fluid saturated bone and conducts currents less easily than in the scalp or CSF. Defects in the skull, burr holes, and foramina may drain stimulation currents with high current densities as described by Agnew and McCreery (1987). However, even when currents drain completely (100%) through a burr-hole, these still disperse greatly in the CSF layer and still leave current densities on the brain surface of several magnitudes below the current densities near stimulation electrodes, where, tissue damage already is unlikely. Current density enhancing effects in foramina of cranial nerves will be less prominent than in burr holes, while neither visual nor auditory effects due to TES are reported in the literature.

The relatively thin skull and relatively thick CSF layer in neonates outbalance their influence on TES thresholds, which make them comparable to adults. It is concluded that skull defects are of no harm to brain tissue and minor significance on stimulation thresholds.

Direct cortical stimulation and excitotoxicity

DCS or neural stimulation is often performed by spherical ball-probe tips with diameters between 1 and 3 mm. For motor stimulation, short pulse trains are used. The reported maximum stimulation intensities for double-pulse DCS motor stimulation is 50 mA (Holsheimer et al., 2007). This is 1/20th of the worst-case condition in TES. When assuming biphasic trains of 8 ppt, 0.1 ms pulse width, and a hemisphere contact surface

(TSCF = 0.5) with a 1 mm diameter the temperature rise at the ball tip surface Δ is equal to 1.35°C. For a diameter of 1.5 mm, ΔT at the ball tip surface is reduced to 0.33°C.

These conditions can already be considered as safe without heat drainage. However, most DCS techniques are described as potentially excitotoxic which is based on current densities over 12 µC/cm^2/phase and 6 µC/phase. This includes DCS with continuous 0.5 ms pulses for 2 mm sphere probes (Gordon et al., 1990; MacDonald, 2002) and DCS for MEPs with 2–3 mm diameter cylindric (Sala and Lanteri, 2003; Yamamoto et al., 2004; Szelényi et al., 2005; Abalkhail et al., 2017) or 1 cm^2 disk electrodes (Taniguchi et al., 1993). The exposure times remain too short for cytotoxic effects.

The temperature increase of Penfield stimulation series of 20 mA 0.5 ms biphasic pulses at 60 Hz at a hemispheric stimulation probe of 1 and 2 mm diameters is computed as, respectively, 40.5°C and 2.6°C over 5 s. Without heat drainage, stimulation by the 1 mm ball-tip would be potentially excitotoxic for a thin tissue slice around the hemisphere tip. However, when taking heat drainage into account, thermic excitotoxity is convincingly excluded. This is clearly shown by convolution with a mono-exponential impulse response function with a time constant of 20 ms, which shows a reduction of the temperature increase from 40.5°C to only 0.39°C. In addition, the heat conduction to the surrounding tissue causes a gradual increase of temperature at effective radial distances from the surface of 2 mm by 7.8, 3.6, 1.9, 1.2, and 0.73°C at 20 mA or 1.4, 1.1, 0.65, and 0.41°C at 15 mA for, respectively, ball-tip diameters of 1, 1.5, 2, 2.5 and 3 mm. Lower temperature build-up effects of 0.5–1°C over 120 s, where also heat drainage by blood perfusion becomes evident, are observed in the experimental data of flash RF pulses of Cosman and Cosman (2005). One can conclude a safe use for continuous Penfield DSC without tissue damage. One may consider choosing larger electrode diameters than 1 mm to limit charge and current densities.

It remains unclear what other impacting causes, other than thermal effects may cause excitotoxicity, when current safety limits of charge per phase and charge density per phase are surpassed. These are still is considered as a concern in DCS (McCreery et al., 1990; MacDonald, 2002; Merrill et al., 2005; MacDonald and Deletis, 2008). Experimental animal models clearly demonstrate excitotoxic damage (McCreery et al., 1990) for 50 or 60 Hz biphasic pulse trains lasting hours or days. These long exposure times are 5–7 magnitudes higher than the brief <5 s and very brief pulse trains <30 ms in TES and DCS (MacDonald, 2002). At these long exposure times, pulse charge (Q) and charge density (QD)

in $\mu C/cm^2$ are reciprocal cofactors that determine the injury threshold (McCreery et al., 1990; Merrill et al., 2005). Below these published injury thresholds the cortex tolerates stimulation indefinitely; above it, damage severity increases over the length of stimulation time. In practice, most DCS parameters exceed the experimental injury threshold but exposure times are too short and appear safe. This is also supported by the absence of clinical or histologic evidence of injury (Gordon et al., 1990; MacDonald, 2002; MacDonald and Deletis, 2008; MacDonald et al., 2013). The only human histological study on DCS reported no thermal injury (Gordon et al., 1990). One has a wider choice in stimulus parameters than applied in practice.

Complications from TES muscle contractions

BITE INJURIES

Bite injuries are the most common TES complication with an estimated 0.2% incidence (MacDonald and Janusz, 2002; MacDonald and Deletis, 2008). A higher incidence rate of 6.5% is reported by Yata et al. (2018). All published bite injuries involve C3/4 (Jones et al., 1996; Calancie et al., 1998, 2001; MacDonald, 2006; Duma et al., 2009; Yata et al., 2018).

Although JLS has had bite injuries with electrodes at M1/M2 and in between M1 and M2 placements (unpublished). Masseter and temporalis muscle contractions by stimulation at C3/C4 are stronger than at C1/C2 or Cz/Fz due to the short extracranial stimulation currents pathways to the trigeminal nerves and branches to temporalis muscles. In addition, the condition for direct muscle stimulation adheres in the vicinity near the stimulation electrodes and likely is a dominating factor in the contraction of the temporalis muscle. Activation via the corticobulbar route is expected to evoke less prominent to jaw muscle contraction.

Most injuries are self-healing tongue or lip contusions or lacerations (Fig. 5.8A). One jaw fracture and two armored endotracheal tube ruptures have been reported (Calancie et al., 1998; Calancie et al., 2001; MacDonald, 2006; Duma et al., 2009). Soft bite-blocks or rolled-up gauze between teeth (Fig. 5.8B) are a standard to reduce the chance of injuries (Duma et al., 2009). The C3/C4 montages may require extra attention.

MOVEMENT-INDUCED INJURY

The possibility of injury due to patient movement from TES is a generally recognized concern, although no adverse events have been reported in the literature to date. Movements of the jaw and head most likely result from extracranial stimulation, while movements at thoracic, lumbar, and sacral locations apparently originate from the cortico-spinal axonal route (Hoebink et al., 2014, 2016). Induced movements of the neck at craniocervical and cervical-thoracic levels were stronger at Cz/Fz when compared to C3/C4 and are in the neck about five times stronger than at lumbar or sacral levels. There does not seem to be any significant differences between movements in the lumbar and sacral region when comparing stimulation at C3/C4 to Cz/Fz.

There are strategies to minimize or manage movement (MacDonald, 2002; MacDonald and Deletis, 2008): DCS produces focal MEPs with no generalized twitches. C3–Cz, C4–Cz, C1/2, and midline TES montages limit movement from facial muscles when compared to C3/4. Near-threshold TES intensities might reduce movements but with the effect of increased MEP amplitude variations
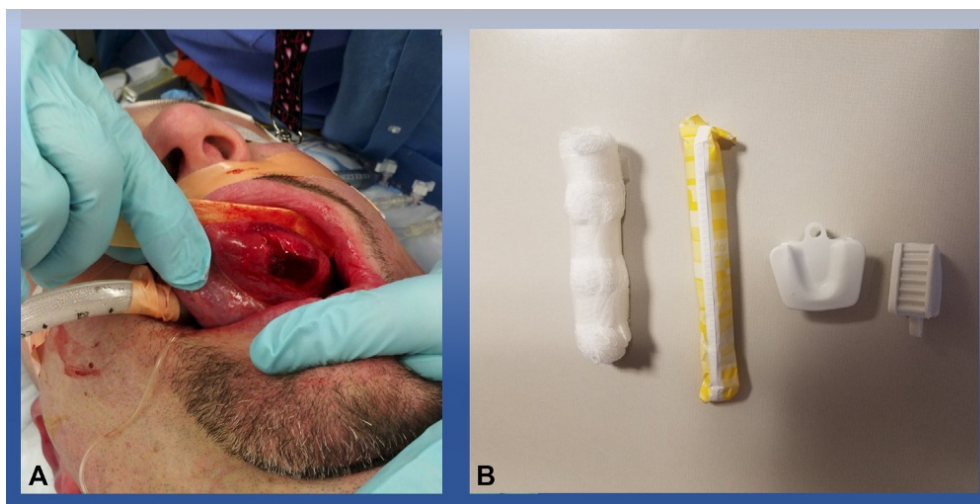

Fig. 5.8. (A) Example of a TES-induced bite injury. (B) Rolled-up gauze between teeth or soft bite-blocks are standard measures for the protection of bite injuries (Shils, with permission).

(Journée et al., 2017). When disturbing movements remain, one relies on careful timing guided by surgical field video and surgeon communication.

Seizures and after discharges

Cortical stimulation may provoke after discharges that may build up to a seizure. 50–60 Hz trains lasting seconds are particularly epileptogenic (MacDonald, 2002). The Penfield technique often elicits after discharges and causes seizures in 5%–20% of patients (Sartorius and Wright, 1997).

Seizures that occur rarely with short TES pulse trains with an estimated 0.03% incidence, are self-limited and free of morbidity (MacDonald, 2002). DCS brief pulse trains have an estimated seizure incidence of 1% (Szelényi et al., 2005).

It is advisable to be prepared for a seizure with anticonvulsants and ice-cold irrigation during DCS. Relative TES contraindications include epilepsy; cortical lesions; skull defects; intracranial vascular clips, shunts, or electrodes; and pacemakers or other implanted bioelectric devices (MacDonald, 2002; MacDonald and Deletis, 2008). There is no proof that any of them increase TES complications and many patients with one or more of these conditions have undergone uneventful MEP monitoring. If the risk of the motor deficit without MEP monitoring outweighs the uncertain additional risk of a relative contraindication, then it is justifiable to proceed.

MEP and implanted devices

Pacemakers, implantable cardioverter defibrillators, (ICD) and implanted neural stimulators are a relative concern for safety when using TES and cautery. However, one case report of a patient with a sick-sinus syndrome showed that the function of pacemakers in DDD mode can show significant interference from fast repeated pulse stimulations for automated threshold finding systems of (NV-M5 NuVasive, San Diego) using extensive series of multi-pulse trains with current increases between 100 and 1200 mA, requiring dozens of seconds (Hayashi, 2016). In contrast to electric elicitable tissue fibers, which are only sensitive for gradients of the electric field, sensors of implanted pacemakers and ICD's remain sensitive for the electric field while the activation function is zero. When from a clinical view, the function of implanted stimulators is not necessary during the monitoring it is advised to uncouple the outputs by turning the devices off and setting the output currents to zero. When all outputs are switched off, or selected in a bipolar mode, no significant currents will flow through a stimulator circuit and human body. It is advised to place all electrodes away from burr-holes of implanted electrodes. When cautery is necessary for the neighborhood of electric conducting parts of an implanted stimulator device, it is strongly advised to use bipolar cautery.

As of the writing of this chapter, there are no published data on the use of the TES with implanted deep brain stimulation (DBS) system. In the authors' experience, TES has been used with sub-thalamic nucleus (STN) DBS leads with no issues. When TES is used with DBS systems, we placed the stimulating leads at M3/M4 to stay away from the lead burr holes that are usually placed anterior to the supplementary motor areas closer to M1/M2. When placing needles in a patient with DBS it is critical to keep all the TES, SEP, and EEG leads away from all DBS components. These components include the burr hole cap and the lead/extension wires that run under the scalp usually a little posterior to the burr holes, although there may be some wire coiling under the burr holes. Additionally, on one side the extension will run down the inside of the scalp to the neck. In older systems, where two implantable pulse generators are used in the chest the wires will run down each side of the neck. When placing stimulation return wires, for example during skull base or posterior fossa procedures, the needles should stay away from the lead and extensions wires to avoid damaging them.

There are three reported cases of TES in patients undergoing spine surgery who had a cochlear implant (Yellin et al., 2016; Abiola et al., 2018) with no reported complications. Pre-operative and post-operative lead impedance and patient audiometry were performed. Overall lead impedance variation was 3% with no significant change in the pre- and post-audiometry data. The patient did not report any changes in hearing post-procedure (Abiola et al., 2018).

Invasive electrode complications

Invasive spinal electrodes carry a small but potentially serious risk of hemorrhagic, traumatic, or infectious complications (MacDonald, 2002; MacDonald and Deletis, 2008). D-wave benefits appear to outweigh these risks for intra-medullary spinal cord tumor surgery (Sala et al., 2006). However, this may not be the case for scoliosis surgery (Ulkatan et al., 2006). Subdural stimulating electrodes slid underneath the skull may cause bleeding, but no morbidity has been reported and the technique might enhance monitoring (Szelényi et al., 2005).

There may be other justifiable indications for invasive techniques that may be an informed consent consideration. The use of needles during interventional procedures where heparin may be used, such as coiling, stenting, or embolic treatment of cranial aneurysms should be limited. The authors have reduced the total number of needles

needed in these procedures to five (C3′, Cz′, and C4′ for SSEP/EEG and M3, M4 for TES). All other electrodes are radiolucent surface "sticky pads" or standard surface stick pads. Gold cup electrodes have been tried but they can interfere with the imaging.

EQUIPMENT-RELATED SAFETY ISSUES

Leakage currents

When powered by AC mains, all medical equipment produces three types of leakage current: (1) chassis leakage current that flows from the device enclosure through the patient or operator to ground or another enclosure part; (2) patient leakage current that flows from patient connections to ground and may originate from an external voltage source on the patient; and (3) patient auxiliary current that flows between patient connections, e.g., impedance testing or amplifier bias (NFPA 99, 2005; IEC 60601-1, 2012). Avoiding excessive transthoracic or direct cardiac conduction of otherwise minor leakage current is critical.

Intraoperative neurophysiologic devices commonly have multiple connections to the patient that create transthoracic paths and add to the total leakage current (IEC 60601-1, 2012). Other electric device connections apply external voltage sources and ground paths such as the electrosurgic devices. Furthermore, internal jugular or subclavian central lines can create potential conductive pathways into the heart. Consequently, the monitoring device cabling, the operator who may be in contact with this equipment, and patient connections should not contact these lines (IEC 60601-1, 2012). Erb's point is a nearby patient connection for IOM that could make contact and may therefore be safest to omit, even though there are no reports of such an event as of the writing of this chapter (MacDonald and Deletis, 2008). Certainly, one must prevent the worst cases of accidental direct cardiac leakage current shocks or power mains voltage at a patient connection.

MEANS OF PROTECTION AGAINST ELECTRIC SHOCK

All medical electric devices must have at least two built-in means of protection against leakage current shocks. These may be protective grounding, insulation, or impedance satisfying detailed technical specifications (IEC 60601-1, 2012).

SINGLE FAULT SAFE

Devices must also be single fault safe, meaning that the failure of one means of protection doesn't cause unacceptable risk (IEC 60601-1, 2012). Single faults arise spontaneously or from the stress of use; a broken power cord ground is a common example. Some single faults trigger a warning, while others are silent and their safety depends on periodic inspection and repair to minimize the chance of a second fault before the next inspection.

LEAKAGE CURRENT LIMITS

Biomedical testing confirms that leakage currents between any accessible part of the device and ground or another accessible part are within safe limits. Intraoperative neurophysiology devices must be safe for external and internal non-cardiac connections. Presently, the relevant IEC alternating current limits in normal and single fault conditions are 100 and 500 µA for individual leakage currents and 500 and 1000 µA for total leakage current (IEC 60601-1, 2012; IEC60601-2-40, 2016). In addition, leakage current must not exceed 5000 µA in the special condition of an external voltage (including power mains) patient connection. This could generate about 0.25 µA at the heart, which still has a low risk of ventricular fibrillation—unless there is a direct cardiac path (IEC 60601-1, 2012). Note that limits undergo periodic revision, and may vary between jurisdictions.

PERIODIC INSPECTION

Device testing must be done after manufacture, installation, signs of damage, repair, and every 6 months or more when indicated by the manufacturer, local rules, or hard use (NFPA 99, 2005). The biomedical engineer must test interconnected devices supplied by one power cord as a unit, as well as custom-built or modified devices. Neglect of periodic testing increases the risk of a seriously hazardous double fault.

POWER CORDS AND LEAD CONNECTORS

To avoid loss of protective grounding, power outlets should be well-constructed without tin soldering that loosens over time, and power cords must be heavy duty with strain relief at both ends and no strain prone right-angle plugs (MDSR, 1979; NFPA 99, 2005). While discouraged, extension cords meeting the same standards may be acceptable (NFPA 99, 2005). Power and extension cord inspection should be part of periodic testing.

Patient leads with unprotected pin connectors can result in electrocution from accidental power contact (MDSR, 1993). Consequently, patient leads must have "touch proof" connectors that cannot make potentially dangerous electric contacts when not seated in their intended receptacles (NFPA 99, 2005; IEC 60601-1, 2012).

Table 5.1 summarizes do's and don'ts recommendations for safe use of intra-operative neuro-physiologic monitoring equipment.

Table 5.1

***Do's and don'ts* recommendations for safety.**

Do's and Don'ts for safety

– Do make sure the bite blocks are placed between the teeth on both sides of the mouth with the tongue between—not under—them.
– Do make sure the needle electrodes are pushed all the way in the skin and tape to secure.
– Do use corkscrew instead of needle electrodes for TES to avoid gradual dislodging from movements of the patient.
– Connect EEG electrodes to a different amplifier box than used for MEP or disconnect these during TES.
– Do make sure the IONM equipment is checked by institutional biomedical engineering.
– Do make sure all implantable devices are set in the "OFF" mode if possible. If not possible, such as for implantable defibrillators and pacemakers, make sure anesthesia knows to watch for arrhythmias during TES stimulation.
– Do use bipolar cautery and stay away from lead burr holes when DBS devices are present.
– In cases where heparin is going to be used try to minimize the number of needle electrodes used. Use sticky pads wherever possible.
– Do prepare anti-convulsants and ice-cold saline for facing epileptic convulsions from Penfield stimulation.
– Do not run electrode cables parallel to the cautery cables.
– Do not run electrode cables parallel (preferably not near) any other electric lines such as EKG lines and central lines.
– Do not reuse needles.
– Do not place the ISO ground near the heart region.

CONCLUSIONS

While intra-operative neuro-physiologic assessment and monitoring improve the safety of patients, the use of the equipment may also introduce new risks of injuries. Knowledge of the hazards and measures for prevention minimizes the risks and makes intra-operative neuro-physiology sufficiently safe in experts' hands.

ACKNOWLEDGMENTS

REFERENCES

Abalkhail TM et al. (2017). Intraoperative direct cortical stimulation motor evoked potentials: stimulus parameter recommendations based on rheobase and chronaxie. Clin Neurophysiol. https://doi.org/10.1016/j.clinph.2017.09.005.

Abiola G et al. (2018). Safe intraoperative neurophysiologic monitoring during posterior spinal fusion in a patient with cochlear implants. Otol Neurotol. https://doi.org/10.1097/MAO.0000000000001788.

Agnew WF, McCreery DB (1987). Considerations for safety in the use of extracranial stimulation for motor evoked potentials. Neurosurgery. https://doi.org/10.1097/00006123-198701000-00030.

Berends HI, Journée HL (2018). Influence of the montage of stimulation electrodes for intraoperative neuromonitoring during orthopedic spine surgery. J Clin Neurophysiol 35 (5): 419. https://doi.org/10.1097/WNP.0000000000000498.

Bourdillon P et al. (2016). Stereo-electro-encephalography – guided radiofrequency thermocoagulation: from in vitro and in vivo data to technical guidelines. World Neurosurg. https://doi.org/10.1016/j.wneu.2016.06.095.

Calancie B et al. (1998). "Threshold-level" multipulse transcranial electrical stimulation of motor cortex for intraoperative monitoring of spinal motor tracts: description of method and comparison to somatosensory evoked potential monitoring. J Neurosurg 88: 457–470. https://doi.org/10.3171/jns.1998.88.3.0457.

Calancie B et al. (2001). Threshold-level repetitive transcranial electrical stimulation for intraoperative monitoring of central motor conduction. J Neurosurg 95 (2): 161. https://doi.org/10.3171/spi.2001.95.2.0161.

Carslaw HS, Jaeger JC (1959). Conduction of heat in solids, second edn. Oxford University Press.

Cosman ER, Cosman ER (2005). Electric and thermal field effects in tissue around radiofrequency electrodes. Pain Med. https://doi.org/10.1111/j.1526-4637.2005.00076.x.

Duma A, Novak K, Schramm W (2009). Tube-in-tube emergency airway management after a bitten endotracheal tube caused by repetitive transcranial electrical stimulation during spinal cord surgery. Anesthesiology. https://doi.org/10.1097/ALN.0b013e3181b8f694.

Faes TJ et al. (1999). The electric resistivity of human tissues (100 Hz-10 MHz): a meta-analysis of review studies. Physiol Meas 20 (4): R1–10. https://doi.org/10.1088/0967-3334/20/4/201.

Gordon B et al. (1990). Parameters for direct cortical electrical stimulation in the human: histopathologic confirmation. Electroencephalogr Clin Neurophysiol. https://doi.org/10.1016/0013-4694(90)90082-U.

Hayashi K (2016). Unpredictable interference of new transcranial motor-evoked potential monitor against the implanted pacemaker. J Clin Anesth 35: 230–231. https://doi.org/10.1016/j.jclinane.2016.09.002.

Hoebink E et al. (2014). 11. Evoked movements in transcranial electrical stimulation on 4 locations of the body at different stimulation electrode montages and stimulation paradigms. Clin Neurophysiol. https://doi.org/10.1016/j.clinph.2013.12.014.

Hoebink EA et al. (2016). Movement along the spine induced by transcranial electrical stimulation related electrode positioning. Spine. https://doi.org/10.1097/BRS.0000000000001495.

Holsheimer J et al. (2007). The role of intra-operative motor evoked potentials in the optimization of chronic cortical stimulation for the treatment of neuropathic pain. Clin Neurophysiol. https://doi.org/10.1016/j.clinph.2007.07.015.

IEC 60601-1 (2012). IEC 60601–1 (Ed. 3.1): medical electrical equipment—part 1: general requirements for basic safety and essential performance [Internet]. Available at: www.iec.ch.

IEC60601-2-40 (2016). IEC 60601–2-40 (Ed. 2.0): Medical electrical equipment—part 2–40: particular requirements for the basic safety and essential performance of electromyographs and evoked response equipment [Internet]. International.

ITIS database (2019a). Heat-transfer-rate(perfusion) assessed 15 Dec 2019. https://itis.swiss/virtual-population/tissue-properties/database/heat-transfer-rate/.

ITIS database (2019b). Heat-transfer-capacity. assessed 15 Dec 2019. https://itis.swiss/virtual-population/tissue-properties/database/heat-capacity/Electrotechnical Commission. Available at: www.iec.ch.

Jones SJ et al. (1996). Motor evoked potential monitoring during spinal surgery: responses of distal limb muscles to transcranial cortical stimulation with pulse trains. Electroencephalogr Clin Neurophysiol 100 (5): 375–383.

Journée HL et al. (2003). Failure of Digitimer's D-185 transcranial stimulator to deliver declared stimulus parameters. Clin Neurophysiol 114 (12). https://doi.org/10.1016/S1388-2457(03)00257-8.

Journée HL, Polak HE, de Kleuver M (2004). Influence of electrode impedance on threshold voltage for transcranial electrical stimulation in motor evoked potential monitoring. Med Biol Eng Comput 42 (4): 557–561. https://doi.org/10.1007/BF02350999.

Journée HL, Berends HI, Kruyt MC (2017). The percentage of amplitude decrease warning criteria for transcranial MEP monitoring. J Clin Neurophysiol 34 (1): 22–31. https://doi.org/10.1097/WNP.0000000000000338.

MacDonald DB (2002). Safety of intraoperative transcranial electrical stimulation motor evoked potential monitoring. J Clin Neurophysiol. https://doi.org/10.1097/00004691-200210000-00005.

MacDonald DB (2006). Intraoperative motor evoked potential monitoring: overview and update. J Clin Monit Comput. https://doi.org/10.1007/s10877-006-9033-0.

MacDonald DB, Deletis V (2008). Safety issues during surgical monitoring. In: MR Nuwer (Ed.), Handbook of clinical neurophysiology, 8th edn. Elsevier, pp. 882–898.

MacDonald DB, Janusz M (2002). An approach to intraoperative neurophysiologic monitoring of thoracoabdominal aneurysm surgery. J Clin Neurophysiol. https://doi.org/10.1097/00004691-200201000-00006.

MacDonald DB et al. (2013). Intraoperative motor evoked potential monitoring—a position statement by the American Society of Neurophysiological Monitoring. Clin Neurophysiol 124 (12): 2291–2316. https://doi.org/10.1016/j.clinph.2013.07.025.

McCreery DB et al. (1990). Charge density and charge per phase as cofactors in neural injury induced by electrical stimulation. IEEE Trans Biomed Eng. https://doi.org/10.1109/10.102812.

MDSR (1979). Electrical plugs: a compendium of problems [Internet], Medical Device Safety Reports. Available at: www.mdsr.ecri.org.

MDSR (1993). Risk of electric shock from patient monitoring cables and electrode lead wires [Internet]. Available at: www.mdsr.ecri.org.

Merrill DR, Bikson M, Jefferys JGR (2005). Electrical stimulation of excitable tissue: design of efficacious and safe protocols. J Neurosci Methods. https://doi.org/10.1016/j.jneumeth.2004.10.020.

Morano JM, Tung A (2019). Bradycardic arrest during somatosensory-evoked potential monitoring: a case report. A A Pract 13 (12): 461–463.

NFPA 99 (2005). NFPA 99: standards for health care facilities [internet], National Fire Protection Association. Available at: www.nfpa.org.

Oh MY et al. (2001). Deep brain stimulator electrodes used for lesioning: proof of principle. Neurosurgery. https://doi.org/10.1097/00006123-200108000-00018.

Ponder BL et al. (2003). Acute bradycardia as a result of intraoperative transcranial electric motor evoked potential stimulation: a case report. Am J Electroneurodiagnostic Technol. https://doi.org/10.1080/1086508x.2003.11079424.

Rattay F (1986). Analysis of models for external stimulation of axons. IEEE Trans Biomed Eng. https://doi.org/10.1109/TBME.1986.325670.

Sala F, Lanteri P (2003). Brain surgery in motor areas: the invaluable assistance of intraoperative neurophysiological monitoring. J Neurosurg Sci.

Sala F et al. (2006). Motor evoked potential monitoring improves outcome after surgery for intramedullary spinal cord tumors: a historical control study. Neurosurgery 58: 1129–1143. https://doi.org/10.1227/01.NEU.0000215948.97195.58.

Sartorius CJ, Wright G (1997). Intraoperative brain mapping in a community setting—technical considerations. Surg Neurol 47: 380–388. https://doi.org/10.1016/S0090-3019(96)00340-0.

Strickland BA et al. (2013). Radiofrequency lesioning through deep brain stimulation electrodes: a pilot study of lesion geometry and temperature characteristics. J Clin Neurosci. https://doi.org/10.1016/j.jocn.2013.03.007.

Szelényi A et al. (2005). Motor evoked potential monitoring during cerebral aneurysm surgery: technical aspects and comparison of transcranial and direct cortical stimulation. Neurosurgery 57: 331–338. https://doi.org/10.1227/01.NEU.0000176643.69108.FC.

Szelényi A, Kothbauer KF, Deletis V (2007). Transcranial electric stimulation for intraoperative motor evoked potential monitoring: stimulation parameters and electrode montages. Clin Neurophysiol 118: 1586–1595.

Szelényi A et al. (2013). Experimental study of the course of threshold current, voltage and electrode impedance during stepwise stimulation from the skin surface to the human cortex. Brain Stimul 6 (4). 482–489. https://doi.org/10.1016/j.brs.2012.10.002.

Taniguchi M, Cedzich C, Schramm J (1993). Modification of cortical stimulation for motor evoked potentials under general anesthesia: technical description. Neurosurgery 32 (2): 219–226.

Tsutsui S, Yamada H (2016). Basic principles and recent trends of transcranial motor evoked potentials in intraoperative neurophysiologic monitoring. Neurol Med Chir. https://doi.org/10.2176/nmc.ra.2015-0307.

Tsutsui S et al. (2015). Augmentation of motor evoked potentials using multi-train transcranial electrical stimulation in intraoperative neurophysiologic monitoring during spinal surgery. J Clin Monit Comput 29: 35–39. https://doi.org/10.1007/s10877-014-9565-7.

Ulkatan S et al. (2006). Monitoring of scoliosis surgery with epidurally recorded motor evoked potentials (D wave) revealed false results. Clin Neurophysiol. https://doi.org/10.1016/j.clinph.2006.05.021.

Yamamoto T et al. (2004). Intraoperative monitoring of the corticospinal motor evoked potential (D-wave): clinical index for postoperative motor function and functional recovery. Neurol Med Chir. https://doi.org/10.2176/nmc.44.170.

Yata S et al. (2018). Bite injuries caused by transcranial electrical stimulation motor-evoked potentials' monitoring: incidence, associated factors, and clinical course. J Anesth. https://doi.org/10.1007/s00540-018-2562-0.

Yellin JL et al. (2016). Safe transcranial electric stimulation motor evoked potential monitoring during posterior spinal fusion in two patients with cochlear implants. J Clin Monit Comput 30: 503–506. https://doi.org/10.1007/s10877-015-9730-7.